Journal of Applied Mechanics and Technical Physics, Vol. 40, No. 1, 1999

PROPAGATION OF SHOCK WAVES IN A TWO-PHASE MIXTURE WITH DIFFERENT PRESSURES OF THE COMPONENTS

A. A. Zhilin and A. V. Fedorov

UDC 532.529

The process of propagation of shock waves in two-component mixtures is considered. The studies were performed within the framework of the two-velocity approximation of mechanics of heterogeneous media with account of different pressures of the components. The stability of propagation of all types of stationary shock waves (fully dispersed, frozen-dispersed, dispersed-frozen, and frozen shock waves of two-front configuration) to infinitesimal and finite perturbations is shown numerically, using the method of coarse particles. The problem of initiation of shock waves (the formation of different types of shock waves from stepwise initial data) is solved. Flows in the transonic range relative to the speed of sound in the first component are obtained.

The propagation of shock waves (SW) in two-component mixtures of condensed materials were studied from the viewpoint of mechanics of heterogeneous media for different pressures of the components [1–7]. Materials that satisfy the linear equation of state were considered in different asymptotic approximations for relaxation times of the nonequilibrium processes of equalization of velocities and pressures. Zhilin et al. [6] and Zhilin and Fedorov [7] examined in detail the problem of the structure of stationary shock waves in the mixture in the general case of finite relaxation times. The range of existence of different SW types (of one- and two-front configuration) was determined in the plane of the following parameters: the initial volume concentration of the first phase in the mixture and the SW velocity. In the present paper, we deal with the problems of numerical simulation of the propagation and initiation of these waves within the framework of the one-dimensional nonstationary model of mechanics of heterogeneous media.

1. Physico-Mathematical Formulation of the Problem. To describe the process of propagation of nonstationary shock waves in a heterogeneous mixture of condensed media with different pressures and velocities of the components, we use the equations of mechanics of heterogeneous media. The conservation laws of mass and momentum for each component of the mixture are supplemented by the equation of the m_2-transfer and equations of state and are written in the following dimensionless form:

$$\frac{\partial \rho_1}{\partial t}+\frac{\partial \rho_1 u_1}{\partial x}=0,\quad \frac{\partial \rho_2}{\partial t}+\frac{\partial \rho_2 u_2}{\partial x}=0,\quad \frac{\partial \rho_1 u_1}{\partial t}+\frac{\partial \rho_1 u_1^2}{\partial x}=-m_1\frac{\partial P_1}{\partial x}+F_S,$$
$$\frac{\partial \rho_2 u_2}{\partial t}+\frac{\partial \rho_2 u_2^2}{\partial x}=-m_2\frac{\partial P_2}{\partial x}-(P_2-P_1)\frac{\partial m_2}{\partial x}-F_S,\quad \frac{\partial m_2}{\partial t}+u_2\frac{\partial m_2}{\partial x}=R, \tag{1.1}$$
$$m_1=1-m_2,\quad P_1=\rho_1/m_1-1,\quad P_2=a^2(\rho_2/m_2-\bar{\rho}).$$

Here ρ_i, u_i, P_i, and m_i are the mean density, velocity, pressure, and volume concentration of the ith component of the mixture, $F_S=m_1\rho_2(u_2-u_1)/\tau_S$ is the Stokes force, $\tau_S=2\bar{\rho}/(9\mu_1)$ is the time of Stokes relaxation of velocities, $R=m_1m_2(P_2-P_1)/\tau_{m_2}$ is the function that describes the transfer of the solid phase, $\tau_{m_2}=2\rho_{22,0}a_2r/(\rho_{11,0}a_1^2)\approx 2\mu_2$ is the time of pressure relaxation in the components of the mixture, μ_i is the

Institute of Theoretical and Applied Mechanics, Siberian Division, Russian Academy of Sciences, Novosibirsk 630090. Translated from Prikladnaya Mekhanika i Tekhnicheskaya Fizika, Vol. 40, No. 1, pp. 55–63. January–February, 1999. Original article submitted April 28, 1997.

 0021-8944/99/4001-0046 $22.00

dynamic viscosity of the ith component, $a = a_2/a_1$, $\bar{\rho} = \rho_{22,0}/\rho_{11,0}$, $\rho_i = m_i\rho_{ii}$, ρ_{ii} is the true density of the ith component, and a_i and $\rho_{ii,0}$ are the speed of sound and the true density of the material of the ith component of the mixture. The velocities are normalized to a_1, the densities to $\rho_{11,0}$, the pressures to $a_1^2\rho_{11,0}$, the parameter x to the radius of the solid particles r, the time t to $t_0 = r/a_1$, and the dynamic viscosity μ_i to $a_1\rho_{11,0}r$.

For Eqs. (1.1), the correct problem is the Cauchy problem for the vector of the solution $\varphi(\rho_1, \rho_2, u_1, u_2, m_2)$:

$$\varphi = \varphi_1 \qquad \text{for} \quad t = 0, \tag{1.2}$$

Here φ_1 is the vector of flow parameters at the initial time.

Problem 1. *Stability of SW Propagation.*

We consider a steady SW described by the solution of the boundary-value problem for a system of ordinary differential equations as the initial data [6, 7]. In this case, φ_1 represents

— continuous functions for fully dispersed shock waves,

— discontinuous functions in the first (light) component and continuous functions in the second (heavy) component for frozen-dispersed shock waves,

— continuous functions in the first component and discontinuous functions in the second component for dispersed-frozen shock waves, and

— discontinuous functions in both components for frozen shock waves.

For these initial data, the perturbations of all wavelengths are small, which is caused by using the numerical method of solving the boundary-value problem for a system of ordinary differential equations. The solution of this problem is often treated in the literature as the study of the stability of the stationary propagation of shock waves to infinitesimal perturbations.

We study the propagation of shock waves of the above-mentioned types with a superposition of finite-amplitude perturbations of the following form on each component of the mixture:

$$u_i(x) = u_{i,st}(x)\left(1 + A_i \sin\left(\frac{x - x_{f0,i}}{l_{i,\mathrm{Pr}}}\pi k_i\right)\right). \tag{1.3}$$

Here $u_{i,st}(x)$ is the undisturbed velocity profile, A_i is the amplitude of harmonic perturbation of the ith component, $x_{f0,i}$ is the left boundary of the SW front in the ith component, $l_{i,\mathrm{Pr}}$ is the SW thickness in the ith component according to Prandtl, and k_i is the number of loops on the SW in the ith component. The remaining parameters of the initial state were determined from the conservation laws for the mixture.

Problem 2. *Initiation of a Steady Shock Wave.*

As the function φ_1 in (1.2), we consider the steady solution ahead of the front of an SW propagating with velocity D (the initial state φ_0) and behind the SW front (the final state φ_{fin}). Both states belong to the equilibrium Hugoniot adiabat.

2. Numerical Method of Solution. Problems 1 and 2 were solved by the coarse-particle method of the first order of approximation [8, 9], which was modified to take into account the equation of compacting kinetics (i.e., the equation of m_2-transfer). Therefore, at the first stage of calculation, to determine the flow velocities $\tilde{u}_1$ and $\tilde{u}_2$ intermediate in time, we use equations that depend not only on P, but also on P_1 and are written in the form

$$\tilde{u}_{1j} = u_{1j} - \frac{m_{1j}}{\rho_{1j}}\frac{\Delta t}{\Delta x}(P_{1j+1/2} - P_{1j-1/2}),$$

$$\tilde{u}_{2j} = u_{2j} - \frac{1}{\rho_{2j}}\frac{\Delta t}{\Delta x}(P_{j+1/2} - P_{j-1/2}) + \frac{m_{1j}}{\rho_{2j}}\frac{\Delta t}{\Delta x}(P_{1j+1/2} - P_{1j-1/2}).$$

The difference equations have the first-order accuracy in time and space.

At the second stage, the densities of mass and momentum fluxes are usually calculated using a relation with approximation viscosity, which allows the shock-capturing calculation without a significant smearing of the SW front.

At the third and final stage, we find the fields of the flow parameters $\hat{\rho}_i$ and $\hat{u}_i$ at the time $\hat{t} = t + \Delta t$. The volume concentration of the mixture $\hat{m}_2$ at the new time layer is determined from the difference equation

$$\hat{m}_{2j} = \frac{1}{\hat{\rho}_{2j}}\left\{(\rho_2 m_2)_j - \frac{\Delta t}{\Delta x}[(\rho_2 m_2 \tilde{u}_2)_{j+1/2} - (\rho_2 m_2 \tilde{u}_2)_{j-1/2}] + R\rho_{2j}\Delta t\right\},$$

where $R = m_{1j}m_{2j}(P_{2j} - P_{1j})/\tau_{m_2}$.

The boundary of stability of the resultant difference scheme is determined by the Courant–Friedrichs-Lévy condition adapted to a multiphase flow of the mixture:

$$\Delta t < \Delta x/|U_*|.$$

Here $U_* = C_{ef} + u_*$ (u_* is the maximum velocity of wave propagation over the cells).

3. Discussion of Numerical Results. *Stability of Propagation of Shock Waves of Different Types* (Problem 1). We consider the propagation of different SW types obtained by Zhilin and Fedorov [7] for a self-similar flow of the mixture in the unsteady approximation.

(1) For $D = -1.5$ and small values of m_{10}, the steady formulation yields a fully dispersed flow in both components of the mixture. In Problem 1, constant equilibrium values of the parameters of the mixture are maintained at the right boundary of the flow domain; therefore, a dispersed SW with monotonic profiles of velocities and pressures of the components propagates steadily to the left. In calculations, these profiles move steadily with a constant velocity and remain monotonic for $t = 100$, 300, and 500.

It is shown [7] that an increase in the volume concentration of the light component of the mixture changes the flow type from fully dispersed to frozen-dispersed. The new type of flow is characterized by an internal SW in the first phase, but it is continuous in the second phase. The flow steadiness is lost in the initial period of calculation, but then the flow stabilizes again with the same profile (the time of stabilization is $t < 10$). Depending on the value of m_{10}, the shock wave is slightly smeared (from three to five cells). After that, the propagating wave retains a steady configuration of the frozen-dispersed SW. Figure 1 shows the velocity profiles of the components at the times $t = 0$, 10, 30, and 50 for $D = -1.5$ and $m_{10} = 0.95$.

(2) As the SW velocity increases ($D = -2.5$), the initial flow is a fully dispersed SW with a monotonic ($m_{10} = 0.1$) or nonmonotonic ($m_{10} = 0.3$ and 0.5) velocity profile in the light component. As in the case $D = -1.5$, a steady dispersed SW propagates to the left. The velocity profile in the first component is nonmonotonic, and the minimum value is lower than the velocity of the mixture in the final equilibrium state.

As the water content in the mixture (i.e., m_{10}) increases, the flow is reconstructed: a shock wave appears in the first phase. For $D = -2.5$ and $m_{10} = 0.7$ and 0.9, the shock wave propagates steadily with a constant velocity. The shock is slightly smeared because of the method of solution.

(3) As the SW velocity increases ($D = -3.3$ and $m_{10} = 0.4$), the flow with a frozen SW is observed at $t = 0$ in the second component, and a dispersed flow with a nonmonotonic velocity profile is observed in the first component of the mixture. An analysis of the pressure profile of the second component shows that the first shock is also slightly smeared because of the method of solution and the wave propagates steadily with velocity $D = -3.3$.

By increasing the volume concentration $m_{10} = 0.7$ and 0.9 for the same value $D = -3.3$, we pass to the region of existence of a frozen SW of the two-wave structure. At $t = 0$, the flow is characterized by a bow shock wave in the heavy component and by an internal shock wave in the light component. The flow is initially unsteady, but stabilizes with time. The flow in the second component with the front discontinuity is formed somewhat faster than in the first component. After that, a stable steady propagation of the initial two-wave configuration is observed.

We note some characteristic features of the numerical calculation of propagation of different shock-wave types. If we have a discontinuous flow, a drop in the velocity of the light component appears in the solution at first, which causes a change in the remaining parameters behind the SW front. Then the parameters of the mixture become more smooth in the region considered. A decrease in the step in space leads to a more dramatic reduction of the zone of flow stabilization than a decrease in the time step.

Stability of the Shock Wave to Finite Perturbations. By superimposing finite perturbations of the type

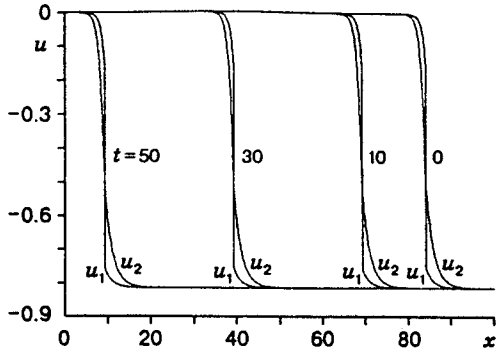

Fig. 1

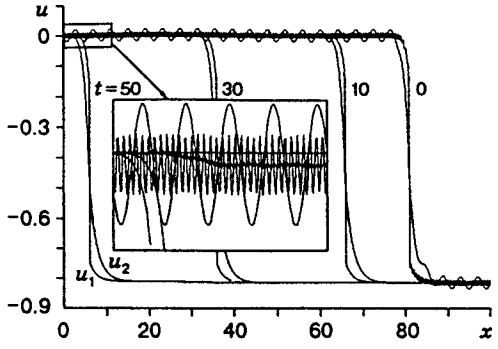

Fig. 2

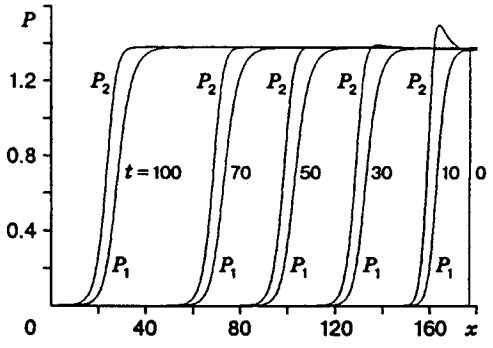

Fig. 3

(1.3) on the shock waves of the examined types, it was found that the profiles of velocities and, hence, of pressures of the components rapidly become stable and propagate with velocity D. Figure 2 shows the process of flow stabilization with perturbations superimposed on the initial data for $D = -1.5$ and $m_{10} = 0.95$. The following features were noted in the calculations:

— An increase in the frequency of perturbations in one of the components leads to an insignificant increase in the time of flow stabilization;

— An increase in the amplitude of harmonic perturbation of the components leads to a proportional increase in the time necessary to obtain a steady flow;

— The time of flow stabilization t_{stab} increases with increasing initial parameters of the mixture (D and m_{10}).

Initiation of Shock Waves (Problem 2).

(1) Stepwise initial data with $m_{10} = 0.2$ form a dispersed SW with velocity $D = -1.5$. The process of formation of such an SW lasts from $t = 0$ to $t = 300$. For $t = 100$, some deviations of the desired profile from that obtained at $t = 300$ are seen (especially in regions adjacent to the initial and final equilibrium states). A further increase in integration time ($t = 300$, 500, 700, and 1000) shows that the profiles of velocities and pressures of the components become stable. As m_{10} increases, the duration of the SW formation decreases. Thus, for $m_{10} = 0.5$, the period of flow stabilization decreases to the interval $t = 0$–100.

An increase in m_{10} to 0.6 leads to flow reconstruction: an internal SW appears in the light component. The amplitude of this wave is very small, and it was difficult to determine its position in the steady problem [7]. In our case, the pressure of the second component exceeds the equilibrium value at the initial stage of flow stabilization, but this peak gradually disappears. The process of formation of this type of flow ends at $t = 50$, $D = -1.5$, and $m_{10} = 0.6$ (Fig. 3).

For $m_{10} = 0.7$, the pressure in the heavy component behaves nonmonotonically, and one has to take into account the specific features of steady solutions to identify the nonmonotonic features caused by numerical

TABLE1

m_{10}	t_{stab}		
	$D = -1.5$	$D = -2.5$	$D = -3.3$
0.2	300	100	25
0.5	100	50	20
0.7	50	20	15
0.9	30	15	15

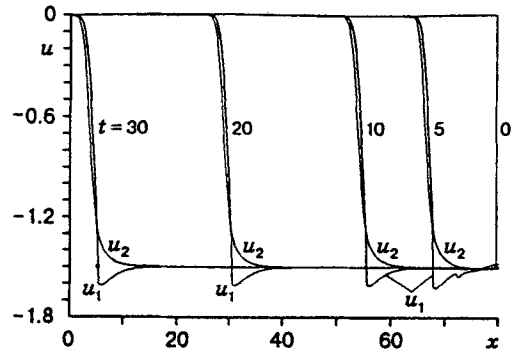

Fig. 4

integration (as, for example, at $m_{10} = 0.6$). As m_{10} increases to 0.85 and 0.95, the SW amplitude increases and the velocity profiles of the components become more and more different. For these values of m_{10}, the flows becomes stable before $t = 30$.

Thus, for m_{10} up to 0.5, the profiles of u_1 and u_2 are very close, and the flow can be considered as equilibrium to a good accuracy. For $m_{10} = 0.6$ and 0.7, an internal SW appears in the first component, the flow is almost equilibrium relative to the velocities ahead of the SW front, and velocity nonequilibrium is observed behind the SW front. As m_{10} increases ($m_{10} = 0.85$ and 0.95), the differences in the velocity profiles of the components are clearly seen in the light component both ahead of the SW front and behind it.

Table 1 shows the dependence of the flow stabilization time of different SW types on the initial SW velocity and volume concentrations of the components. An increase in the volume concentration of the light component leads to a decrease in the zone of flow stabilization, which is caused by inertial properties of the initial materials of the mixture.

(2) As D increases to -2.5, a steady flow is formed faster than for $D = -1.5$. An analysis of the results of flow calculations with $m_{10} = 0.1, 0.3, 0.5, 0.6, 0.7$, and 0.9 shows that they completely coincide with those obtained previously in Problem 1. This allows us to state that, initiating the flow from stepwise initial data, we can obtain velocity and pressure profiles of the same structure as in solving a self-similar problem. Moreover, based on the solution of the SW initiation problem, we can obtain flows whose calculation in the steady-state approximation is difficult because of the presence of internal singular points. The velocity profiles of the components for $D = -2.5$ and $m_{10} = 0.6$ are shown in Fig. 4. The complexity of the solution in the self-similar approximation was due to the necessity of a smooth transition through the speed of sound in the first component. Analyzing the profiles at $t = 20$ and $t = 30$, we can conclude that the transition from the supersonic to the subsonic state in the first component is caused by a small-amplitude internal SW. The fluid is accelerated behind the front of this shock wave, and its velocity profile passes through a_1 at a certain point of the flow. This singular point is nonstationary, and the flow continuously passes to the supersonic state through this point.

We analyze the pattern of transition in a transonic flow in the first phase with a singular point. The change in the velocity in the first phase is described by the ordinary differential equation

$$\frac{dU_1}{d\zeta} = \frac{U_1}{\rho_1}\frac{F_S - \rho_1 R/m_1}{U_1^2 - 1}. \tag{3.1}$$

As the velocity of the first component approaches the speed of sound, a gradient catastrophe occurs in the first phase. Equating the numerator in Eq. (3.1) to zero at $U_1 = 1$, we find that the velocity U_2 in the heavy component satisfies the equation

$$F(U_2) = U_2^5 C_2^3 \tau_{m_2} - U_2^4 C_2^2 [\tau_{m_2}(C_2 + 2C_3 + 2a^2\bar{\rho} - 4C_1) - 2CC_1\tau_S]$$
$$+U_2^3 C_2 [\tau_{m_2}\{(C_3 + a^2\bar{\rho} - 2C_1)^2 + 2C_2(C_3 + a^2\bar{\rho} - 2C_1) + 2a^2C_2^2\}$$

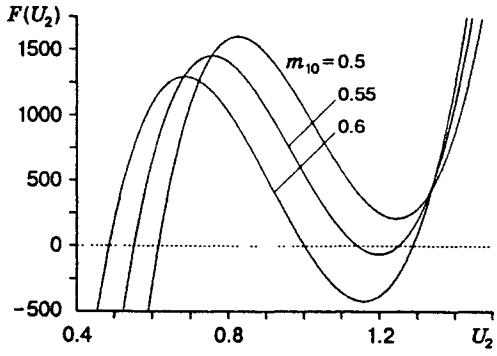

Fig. 5

TABLE 2

m_{10}	$U_0 = 2.5$				$U_0 = 3.3$			
	U_2^{I}	U_2^{II}	U_2^{III}	U_{fin}	U_2^{I}	U_2^{II}	U_2^{III}	U_{fin}
0.35	0.7877	—	—	1.4638	0.7611	—	—	1.5022
0.3715	0.7653	—	—	1.4195	0.7393	1.5616	1.5675	1.4564
0.40	0.7342	—	—	1.3625	0.7092	1.4571	1.5939	1.3970
0.45	0.6762	—	—	1.2664	0.6537	1.3354	1.5891	1.2963
0.50	0.6147	—	—	1.1745	0.5950	1.2247	1.5853	1.1989
0.52	0.5893	—	—	1.1388	0.5708	1.1818	1.5854	1.1607
0.5396	0.5641	1.2042	1.2069	1.1043	0.5467	1.1401	1.5867	1.1237
0.55	0.5506	1.1405	1.2486	1.0862	0.5337	1.1182	1.5879	1.1042
0.58	0.5112	1.0511	1.2761	1.0346	0.4959	1.0551	1.5936	1.0483
0.60	0.4846	1.0012	1.2862	1.0008	0.4703	1.0131	1.5993	1.0115
0.61	0.4712	0.9774	1.2906	0.9841	0.4574	0.9222	1.6029	0.9932

$$-2CC_1\tau_S(2C_3+1+a^2\bar{\rho}-3C_1)] - U_2^2[\tau_{m_2}C_2\{(C_3+a^2\bar{\rho}-2C_1)^2$$
$$+2a^2C_2(C_3+a^2\bar{\rho}-2C_1+C_2)\} - 2CC_1\tau_S\{(C_3+1-2C_1)(C_3+a^2\bar{\rho}-C_1)+C_2^2a^2\}]$$
$$+U_2a^2C_2[\tau_{m_2}C_2(C_2a^2+2C_3+2a^2\bar{\rho}-4C_1) - 2CC_1\tau_S(C_3+1-C_1)] - \tau_{m_2}C_2^3a^4 = 0, \qquad (3.2)$$

where $C = 1 - a^2\bar{\rho}$, $C_i = \rho_{i0}U_0$, and $C_3 = (C_1 + C_2)U_0$. This equation has one real root U_2^{I} in the interval from 0 to 1. It has no physical sense and is not considered in what follows.

The behavior of the function $F(U_2)$ versus the parameter m_{10} for $U_0 = 2.5$ is plotted in Fig. 5. We can see that two more roots of Eq. (3.2) appear. Thus, a U-shaped branch of $F(U_2)$ is located above the abscissa axis at $m_{10} = 0.5$, which goes down as m_{10} increases and touches the axis at $m_{10} \approx 0.5396$. Two multiple roots appear: U_2^{II} and U_2^{III}. A further increase in the volume concentration of the light component leads to the appearance of two more roots. As m_{10} increases, the values of U_2^{II} shift to smaller U_2 and the values of U_2^{III} to greater U_2. The numerical values of the roots are listed in Table 2.

The conducted calculation of the unsteady problem shows that only the second root U_2^{II} is physically realized in the flow. A flow with a short-time outcome into the subsonic region exists at $m_{10} > m_{1*}$ (m_{1*} is the volume concentration for which $U_{1,\min} = 1$) and breaks down when the final velocities reach unity.

Thus, for the initial velocity $U_0 = 2.5$, the transonic flow region begins at $m_{10} \approx 0.53$ and ends at $m_{10} \approx 0.6005$. It should be noted that, after the flow with the sonic final state in the first phase $U_1 = U_2 = U_{\mathrm{fin}} = 1$ is obtained, the subsequent motions of the mixture with increasing m_{10} have a subsonic final state in both components. The analysis confirms that it is possible to pass continuously from the subsonic to the supersonic branch of the solution.

We summarize the above discussion about the emergence of flow with a weak SW in the transonic range. For $D = -2.5$ and small m_{10}, the final state is supersonic in the first phase, and the velocity profile is monotonic. As the content of fluid in the mixture increases, a local minimum appears in the profile $u_1(x)$,

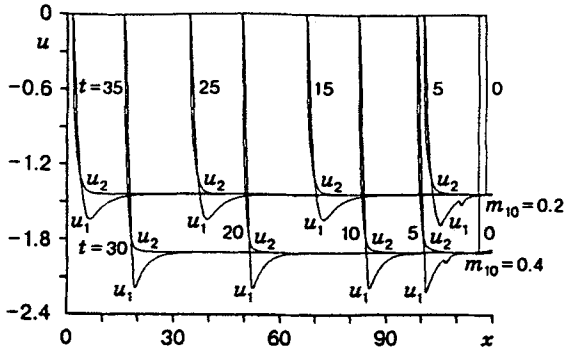

Fig. 6

which approaches the speed of sound in the first phase with increasing m_{10}. There exists a certain value $m_{10} = m_{1*}$ for which $u_{1,\min} = a_1 + D$ and $u_{\text{fin}} > a_1 + D$. A further increase in m_{10} in the stationary approach leads to a gradient catastrophe. This indicates that it is necessary to introduce an SW after which the flow passes continuously through the speed of sound in the first phase, i.e., through an internal singular point (the second-phase velocities for various m_{10} are listed in Table 2). Figure 4 shows the formation of this type of flow for $D = -2.5$ and $m_{10} = 0.6$. A steady flow with an internal SW in the transonic range is formed at $t = 20$ (the internal SW is marked by the dot in the profile of u_1). The subsonic region is characterized by the fact that $u_1(x)$ has a local minimum. As the fluid concentration increases, the position of this minimum approaches the SW front, and the SW amplitude increases. Unsteady calculations of these types of flow demonstrated the stability of their propagation.

(3) As D increases to -3.3, the flow for all m_{10} has a bow SW in the second component. Figure 6 illustrates the process of flow stabilization for $m_{10} = 0.2$ and 0.4. We can trace the formation of the bow SW whose amplitude slightly fluctuates at the initial stage of flow stabilization. We note that the monotonically decreasing profile of the velocity u_2 in the flow with the bow SW is formed faster than the nonmonotonic profile of the velocity u_1 of the first component.

For $m_{10} = 0.5$, a flow that enters the transonic region is formed. For the SW with the propagation velocity $D = -3.3$, the width of the existence region of the transonic flow increases with changing m_{10}. The conducted calculations show that the transonic region begins at $m_{10} \approx 0.43$ and ends at $m_{10} \approx 0.6063$. Some numerical values of the roots of Eq. (3.2) are listed in Table 2, and the characteristic features of the qualitative behavior are similar to the case described for $D = -2.5$.

For $m_{10} = 0.7$ or $m_{10} = 0.9$, a shock wave of two-front configuration with a bow SW in the second component and an internal SW in the first component is formed. As in the previously considered problem of flow stabilization, the flow with the front discontinuity in the second phase is formed faster than the flow with the internal discontinuity in the first phase. We note that the velocities and pressures of the components at a large distance from the SW structure formed are slightly different from the values of these parameters in the final state determined analytically, which is due to the calculation technique.

Conclusions. Based on numerical simulation of unsteady problems of SW propagation in a heterogeneous mixture of condensed media with different pressures and velocities, the following conclusions are drawn.

— The steady dispersed, frozen-dispersed, dispersed-frozen, and fully frozen shock waves are stable to infinitesimal and finite perturbations.

— From the initial data in the form of a step, which is the initial and final states on the equilibrium Hugoniot adiabat, flows with shock waves of the above-mentioned configurations are formed with time.

— There exists a transonic motion of the mixture in the form of a frozen-dispersed SW with a continuous transition through the speed of sound in the first phase.

REFERENCES

1. A. V. Fedorov, "Mathematical description of the flow of a mixture of condensed materials at high pressures," in: *Physical Gas Dynamics of Reactive Media* [in Russian], Nauka, Novosibirsk (1990), pp. 119–128.
2. A. V. Fedorov, "Shock-wave structure in a mixture of two solids (a hydrodynamic approximation)," *Model. Mekh.*, **5(22)**, No. 4, 135–158 (1991).
3. A. V. Fedorov, "Shock-wave structure in a heterogeneous mixture of two solids with equal pressures of the components," in: *Numerical Methods of Solving Problems of Elasticity and Plasticity* (collection of scientific papers) [in Russian], Inst. of Theor. and Appl. Mech., Novosibirsk (1992), pp. 235–249.
4. E. V. Varlamov and A. V. Fedorov, "A traveling wave in a nonisothermal mixture of two solids," *Model. Mekh.*, **5(22)**, No. 3, 14–26 (1991).
5. A. V. Fedorov and N. N. Fedorova, "Structure, propagation and reflection of shock waves in a mixture of solids (the hydrodynamic approximation)," *Prikl. Mekh. Tekh. Fiz.*, No. 4, 10–18 (1992).
6. A. A. Zhilin, A. V. Fedorov, and V. M. Fomin, "A traveling wave in a two-velocity mixture of compressible media with different pressures," *Dokl. Ross. Akad. Nauk*, **350**, No. 2, 201–205 (1996).
7. A. A. Zhilin and A. V. Fedorov, "The shock-wave structure in a two-velocity mixture of compressible media with different pressures," *Prikl. Mekh. Tekh. Fiz.*, **39**, No. 2, 10–19 (1998).
8. A. A. Gubaidullin, A. I. Ivandaev, and R. I. Nigmatulin, "The modified method of coarse particles for calculation of unsteady wave processes in multiphase dispersed media," *Zh. Vychisl. Mat. Mat. Fiz.*, **17**, No. 6, 1531–1544 (1977).
9. A. I. Ivandaev and A. G. Kutushev, "Numerical simulation of unsteady wave flows of suspensions with identification of the boundaries of two-phase regions and contact discontinuities in the carrier gas," in: *Numerical Methods of Continuum Mechanics* (collected scientific papers) [in Russian], Vol. 14, No. 6, Inst. of Theor. and Appl. Mech.–Comput. Center, Novosibirsk (1983), pp. 58–82.